Arabian Journal of Chemistry (2023) **16**, 104970

King Saud University

**Arabian Journal of Chemistry**

www.ksu.edu.sa
www.sciencedirect.com

ORIGINAL ARTICLE

# Bis-indole based triazine derivatives: Synthesis, characterization, *in vitro* β-glucuronidase anti-cancer and anti-bacterial evaluation along with *in silico* molecular docking and ADME analysis

**Shoaib Khan [a], Wajid Rehman [b,*], Fazal Rahim [b], Rafaqat Hussain [b], Ahmad J. Obaidullah [c], Hadil Faris Alotaibi [d], Mohammed M. Alanazi [c], Muhammad Usman Khan [b], Yousaf Khan [e]**

[a] *Department of Chemistry, Abbottabad University of Science & Technology (AUST) Abbottabad, Pakistan*
[b] *Department of Chemistry, Hazara University, Mansehra 21120, Pakistan*
[c] *Department of Pharmaceutical Chemistry, College of Pharmacy, King Saud University, Riyadh 11451, Saudi Arabia*
[d] *Department of Pharmaceutical Sciences, College of Pharmacy, Princess Nourah bint Abdulrahman University, P.O. Box 84428, Riyadh 11671, Saudi Arabia*
[e] *Department of Chemistry, COMSATS University Islamabad, 45550, Islamabad, Pakistan*

Received 16 March 2023; accepted 27 April 2023
Available online 5 May 2023

**KEYWORDS**

Indole;
Triazine synthesis;
SAR;
β-Glucuronidase;
Molecular docking & ADME

**Abstract** The present work described the synthetic procedure adopted for the synthesis of bis-indole-based triazine derivatives *via* a series of reactions. All the compounds were synthesized through a stepwise reaction. After being confirmation through thin-layer chromatography (TLC) these compounds were characterized through various spectroscopic techniques including $^{1}$HNMR, $^{13}$CNMR and HREI-MS and evaluated against beta-glucuronidase in the presence of standard drug D-saccharic acid 1,4 lactone ($IC_{50}$ = 31.2 ± 1.0 μM). Most of the synthesized derivatives were found with better to good inhibitory potentials ($IC_{50}$ = 5.30 ± 2.0 μM to 33.10 ± 1.0 μM). SAR explains better results of analogs due to the presence of varied substituents on the aromatic rings. In this regard, the excellent potential was shown by analogs **1, 3, 6, 8** and **9** with $IC_{50}$ = 5.30 ± 2.0, 7.10 ± 4.0, 6.10 ± 3.0, 8.40 ± 1.0 and 7.20 ± 3.0 μM respectively). In addition, all the synthesized analogs were evaluated for anti-cancer and anti-bacterial (*E. coli)* activities in which the targeted compounds were found with significant potentials in the presence of standard drugs

* Corresponding author.
E-mail address: sono_waj@yahoo.com (W. Rehman).
Peer review under responsibility of King Saud University.

Production and hosting by Elsevier

https://doi.org/10.1016/j.arabjc.2023.104970

Tetrandrineb ($IC_{50}$ = 1.37 ± 0.10 μM) and streptomycin respectively. These derivatives were further subjected to molecular docking studies in order to investigate better binding sites with distance. Additionally, ADME properties for the synthesized compounds were also explored the drug like properties of the synthesized compounds.



## 1. Introduction

The enzyme beta-glucuronidase catalyzes the glycosaminoglycans in the cell membrane as well as the extracellular matrix of both cancerous and healthy cells. The proliferation, invasion, and metastasis of cancer cells are all impacted by this catalysis (Khan et al., 2011; Chojnowska et al., 2011). The rise in β-glucuronidase activity is what causes liver cancer, colon carcinoma, and neoplastic bladder (Szajda et al., 2008; Kim & Jin 2001; Cheng et al., 2012; Zalewska-Szajda et al., 2018). In real-time monitoring, therapeutic therapy, early-stage diagnostics, and as a tumor marker, lucuronidase has been employed as a key tool (Juan et al., 2009; Murdter et al., 2002). Numerous diseases, including epilepsy (Falkenbach et al., 1993) and other physiological disorders, are linked to high levels of β-glucuronidase. Increased levels of β-glucuronidase result in liver injury, which is a significant problem worldwide (Byass 2014). The accumulation of glycosaminoglycans with glucuronic acid residues, which results in lysosomal storage in the brain, is the cause of mucopolysaccharidosis type VII (MPSVII, also known as Sly syndrome), which is brought on by a GUS deficiency in the human body (Hassan et al., 2013; Naz et al., 2013). Inhibiting this enzyme is crucial for preventing such a physiological problem. One of the key areas in medicinal chemistry is the study of heterocyclic molecules. They hold a significant place in the structures of many different natural products. Indole, one of the most useful structures, has drawn a lot of interest due to its pharmacological action and has been regarded as an essential scaffold (Cacchi & Fabrizi 2005; Imran et al., 2015; Elsonbaty et al., 2021). Several compounds based on indoles have been studied for their potential anticancer properties (Dadashpour & Emami 2018). In recent years, indole derivatives have become extremely important drugs. They are widely known for their important biological actions, including their cytotoxic, anti-bacterial, antidiabetic, and anti-inflammatory effects (Sravanthi & Manju 2016; Prakash et al., 2018; Singh & Singh 2018; Goyal et al., 2018). Our research group also works on the varied synthetic procedures of varied heterocyclic compounds (Khan et al., 2022; Khan et al., 2022; Khan et al., 2022; Khan et al., 2022; Khan et al., 2022; Hussain et al., 2022; Mumtaz et al., 2022; Khan et al., 2022; Hussain et al., 2022; Khan et al., 2023; Khan et al., 2022; Adalat et al., 2023; Khan et al., 2022; Khan et al., 2022).

In perspective of above details, in the current study we have planned to synthesize the novel bis-indole based triazine derivatives their characterization, beta-glucuronidase, anti-cancer and anti-bacterial activity, molecular docking and ADME-studies.

## 2. Results and discussion

### 2.1. Chemistry

Bis-indole bearing di-ketone moiety (**I**) was mixed along with thiosemicarbazide in ethanol, and the reaction mixture was refluxed condition for about 8hrs in the presence of potassium carbonate, afforded six-membered hydrazine bearing thiol group as an intermediate moiety (**II**) (Abdel-Rahman et al., 2015). This intermediate moiety (**II**) were further mixed with varied substituted phenacyl bromide in ethanol in the presence of triethylamine ($ET_3N$) and the reaction mixture were refluxed for about 6hrs to obtain bis-indole-based triazine derivatives (**1–12).** The synthesized derivatives (Scheme 1) (1–12) were collected and washed with n-hexane, given fine powder and were characterized through varied spectroscopic techniques such as $^1$HNMR, $^{13}$CNMR and HREI-MS.

### 2.2. Material and methods

All the chemicals were purchased from Sigma Aldrich, USA. Avance Bruker machine was used to performed NMR experiment. Finnigan MAT-311A (Germany) mass spectrometer was used to recorded high resolution electron impact mass spectra (HR-EIMS). Thin layer chromatography (TLC) was done on pre-coated silica gel aluminium plates (Kieselgel 60, 254, E. Merck, Germany). UV at 254 and 365 nm was used to visualize the chromatograms.

### 2.3. Characterizations of bis-Indole based triazole derivatives (1–12)

#### 2.3.1. 2-((5,6-di(1H-Indol-3-yl)-1,2,4-triazin-3-yl)thio)-1-(4-(trifluoromethyl)phenyl)ethan-1-one (1)

Light yellow, $^1$H NMR (600 MHz, DMSO $d_6$): δ 12.19 (s, 2H, N–H), 8.83 (s, 2H, Indole-H (2A/ 2B)), 8.52 (dd, $J$ = 7.8, 2.4 Hz, 2H, Indole-H 4A/ 4B), 7.94 (dd, $J$ = 8.2, 3.2 Hz, 2H, Indole-H 7A/ 7B), 7.90 (d, $J$ = 7.8 Hz, 2H, Ar-H), 7.62–7.71 (m, 4H, Indole-H (5,6A/ 5,6B)), 7.18 (d, $J$ = 6.9 Hz, 2H, Ar-H), 4.69 (s, 2H, $CH_2$-S); $^{13}$C NMR (150 MHz, DMSO $d_6$): δ 191.9, 182.6, 180.4, 177.6, 177.5, 175.0, 173.2, 171.1, 166.8, 165.6, 164.4, 162.9, 160.4, 160.1, 159.5, 159.3, 159.0, 158.9, 154.5, 150.5, 148.9, 146.6, 146.4, 138.8, 136.8, 135.3, 121.7, 41.6; HREI-MS: $m/z$ calcld for $C_{28}H_{18}F_3N_5OS$, $[M]^+$ 529.0153 Found 529.0121.

#### 2.3.2. 2-((5,6-di(1H-Indol-3-yl)-1,2,4-triazin-3-yl)thio)-1-(3-methyl-4-(trifluoromethyl)phenyl)ethan-1-one (2)

Light green, $^1$H NMR (600 MHz, DMSO $d_6$): δ 12.04 (s, 2H, N–H), 8.52 (s, 2H, Indole-H (2A/ 2B)), 8.78 (dd, $J$ = 7.3, 3.0 Hz, 2H, Indole-H 4A/ 4B), 7.83 (dd, $J$ = 7.8, 3.0 Hz, 2H, Indole-H 7A/ 7B), 7.80 (s, 1H, Ar-H), 7.71–7.79 (m, 4H, Indole-H (5,6A/ 5,6B)), 7.62 (d, $J$ = 7.1 Hz, 1H, Ar-H), 7.07 (d, $J$ = 7.3 Hz, 1H, Ar-H), 4.72 (s, 2H, $CH_2$-S) 3.03 (s, 3H, $CH_3$); $^{13}$C NMR (150 MHz, DMSO $d_6$): δ 196.7, 183.1, 180.9, 179.1, 179.0, 178.6, 176.7, 174.6, 169.3, 168.1, 167.9, 165.4, 163.9, 163.6, 161.5, 160.5, 160.3, 158.2, 157.0, 153.0, 151.4, 149.1, 146.5, 142.8, 140.3, 139.8, 126.2, 38.5, 22.4; HREI-MS: $m/z$ calcld for $C_{29}H_{20}F_3N_5OS$, $[M]^+$ 543.7236 Found 543.7196.

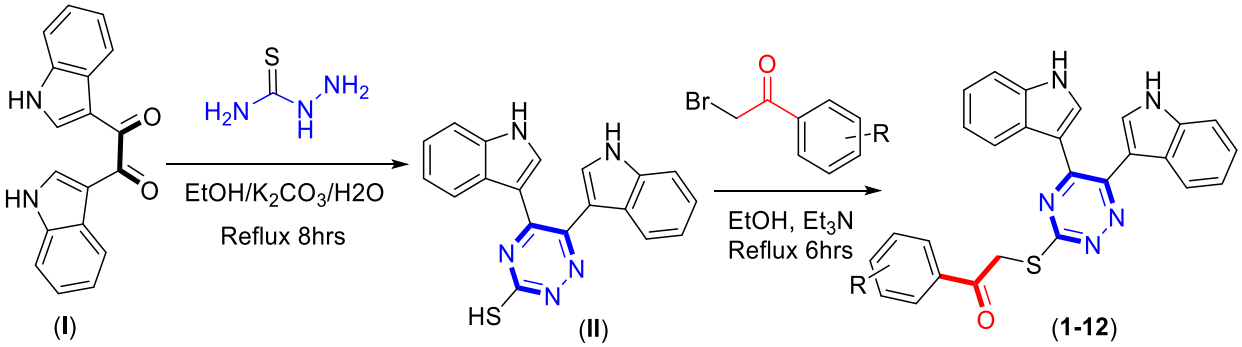


**Scheme 1** Represent adopted route for synthesis of bis-indole based triazine derivatives.

*2.3.3. 2-((5,6-di(1H-Indol-3-yl)-1,2,4-triazin-3-yl)thio)-1-(4-hydroxyphenyl)ethan-1-one (3)*

White, $^{1}$H NMR (600 MHz, DMSO $d_6$): $\delta$ 12.32 (s, 2H, N–H), 10.36 (s, 1H, Ar-OH), 8.78 (s, 2H, Indole-H (2A/ 2B)), 8.65 (dd, $J$ = 7.7, 3.2 Hz, 2H, Indole-H 4A/ 4B), 8.02 (dd, $J$ = 7.3, 2.9 Hz, 2H, Indole-H 7A/ 7B), 7.78–7.86 (m, 4H, Indole-H (5,6A/ 5,6B)), 7.75 (d, $J$ = 6.8 Hz, 2H, Ar-H), 7.53 (d, $J$ = 7.3 Hz, 2H, Ar-H), 4.72 (s, 2H, $CH_2$-S);$^{13}$C NMR (150 MHz, DMSO $d_6$): $\delta$ 195.5, 181.6, 180.7, 179.4, 178.8, 175.8, 174.7, 171.6, 168.7, 166.9, 166.5, 162.7, 160.9, 160.6, 158.4, 157.5, 152.7, 150.4, 149.9, 148.0, 145.6, 144.9, 143.0, 140.3, 139.6, 137.8, 42.5; HREI-MS: $m/z$ calcld for $C_{27}H_{19}N_5O_2S$, $[M]^+$ 477.4328 Found 477.4292.

*2.3.4. 2-((5,6-di(1H-Indol-3-yl)-1,2,4-triazin-3-yl)thio)-1-(3-hydroxy-5-methylphenyl)ethan-1-one (4)*

Light gray, $^{1}$H NMR (600 MHz, DMSO $d_6$): $\delta$ 12.36 (s, 2H, N–H), 10.52 (s, 1H, Ar-OH), 8.43 (s, 2H, Indole-H (2A/ 2B)), 8.39 (dd, $J$ = 7.1, 3.5 Hz, 2H, Indole-H 4A/ 4B), 8.21 (dd, $J$ = 6.9, 3.1 Hz, 2H, Indole-H 7A/ 7B), 7.81–7.89 (m, 4H, Indole-H (5,6A/ 5,6B)), 7.58 (s, 1H, Ar-H), 7.42 (s, 1H, Ar-H), 7.38 (s, 1H, Ar-H), 4.72 (s, 2H, $CH_2$-S) 2.95 (s, 3H, $CH_3$); $^{13}$C NMR (150 MHz, DMSO $d_6$): $\delta$ 188.2, 178.5, 173.1, 170.5, 169.3, 168.8, 167.2, 167.1, 164.7, 161.6, 158.2, 157.6, 157.3, 155.4, 154.9, 151.5, 149.4, 149.2, 149.1, 148.9, 145.4, 144.6, 141.6, 138.1, 137.6, 136.4, 49.4, 37.8; HREI-MS: $m/z$ calcld for $C_{28}H_{21}N_5O_2S$, $[M]^+$ 491.6456 Found 491.6432.

*2.3.5. 2-((5,6-di(1H-Indol-3-yl)-1,2,4-triazin-3-yl)thio)-1-(3-fluoro-4-methylphenyl)ethan-1-one (5)*

Light gray, $^{1}$H NMR (600 MHz, DMSO $d_6$): $\delta$ 12.53 (s, 2H, N–H), 8.42 (s, 2H, Indole-H (2A/ 2B)), 8.72 (dd, $J$ = 7.2, 2.3 Hz, 2H, Indole-H 4A/ 4B), 7.66 (dd, $J$ = 7.0, 3.2 Hz, 2H, Indole-H 7A/ 7B), 7.61 (s, 1H, Ar-H), 7.58–7.65 (m, 4H, Indole-H (5,6A/ 5,6B)), 7.33 (d, $J$ = 7.5 Hz, 1H, Ar-H), 7.17 (d, $J$ = 7.8 Hz, 1H, Ar-H), 4.47 (s, 2H, $CH_2$-S) 3.09 (s, 3H, $CH_3$); $^{13}$C NMR (150 MHz, DMSO $d_6$): $\delta$ 194.5, 186.53 173.2, 172.8, 169.6, 169.4, 166.2, 166.0, 163.3, 162.3, 162.2, 159.7, 153.1, 152.5, 151.6, 148.6, 148.3, 147.4, 147.3, 146.9, 143.2, 141.4, 140.5, 139.8, 138.6, 136.4, 52.6, 38.2; HREI-MS: $m/z$ calcld for $C_{28}H_{20}FN_5OS$, $[M]^+$ 493.5348 Found 493.5307.

*2.3.6. 2-((5,6-di(1H-Indol-3-yl)-1,2,4-triazin-3-yl)thio)-1-(4-fluorophenyl)ethan-1-one (6)*

Light yellow, $^{1}$H NMR (600 MHz, DMSO $d_6$): $\delta$ 12.46 (s, 2H, N–H), 8.83 (s, 2H, Indole-H (2A/ 2B)), 8.59 (dd, $J$ = 7.3, 2.8 Hz, 2H, Indole-H 4A/ 4B), 7.87 (dd, $J$ = 8.3, 3.3 Hz, 2H, Indole-H 7A/ 7B), 7.72 (d, $J$ = 7.2 Hz, 2H, Ar-H), 7.41–7.50 (m, 4H, Indole-H (5,6A/ 5,6B)), 7.23 (d, $J$ = 7.4 Hz, 2H, Ar-H), 4.31 (s, 2H, $CH_2$-S); $^{13}$C NMR (150 MHz, DMSO $d_6$): $\delta$ 190.5, 182.6, 180.7, 176.4, 175.8, 173.5, 168.2, 164.0, 162.3, 160.6, 160.0, 158.6, 157.9, 157.9, 156.4, 153.5, 149.6, 149.5, 147.2, 147.0, 143.0, 142.9, 140.9, 139.7, 138.6, 136.4, 48.8; HREI-MS: $m/z$ calcld for $C_{27}H_{18}FN_5OS$, $[M]^+$ 479.1264 Found 479.1230.

*2.3.7. 2-((5,6-di(1H-Indol-3-yl)-1,2,4-triazin-3-yl)thio)-1-(3-methyl-5-nitrophenyl)ethan-1-one (7)*

Light yellow, $^{1}$H NMR (600 MHz, DMSO $d_6$): $\delta$ 12.43 (s, 2H, N–H), 8.78 (s, 2H, Indole-H (2A/ 2B)), 8.61 (dd, $J$ = 7.1, 3.5 Hz, 2H, Indole-H 4A/ 4B), 8.34 (dd, $J$ = 8.4, 3.5 Hz, 2H, Indole-H 7A/ 7B), 7.86–7.92 (m, 4H, Indole-H (5,6A/ 5,6B)), 7.72 (s, 1H, Ar-H), 7.69 (s, 1H, Ar-H), 7.54 (s, 1H, Ar-H), 4.72 (s, 2H, $CH_2$-S) 2.95 (s, 3H, $CH_3$); $^{13}$C NMR (150 MHz, DMSO $d_6$): $\delta$ 194.2, 177.5, 164.1, 163.4, 161.6, 160.8, 157.2, 157.0, 155.3, 154.6, 154.0, 151.6, 149.9, 148.9, 148.4, 142.5, 142.4, 140.5, 140.2, 140.0, 137.4, 137.2, 136.5, 133.8, 133.6, 130.4, 46.8, 32.6; HREI-MS: $m/z$ calcld for $C_{28}H_{20}N_6O_3S$, $[M]^+$ 520.6373 Found 520.6356.

*2.3.8. 2-((5,6-di(1H-Indol-3-yl)-1,2,4-triazin-3-yl)thio)-1-(4-nitrophenyl)ethan-1-one (8)*

Light yellow, $^{1}$H NMR (600 MHz, DMSO $d_6$): $\delta$ 12.58 (s, 2H, N–H), 8.61 (s, 2H, Indole-H (2A/ 2B)), 8.58 (dd, $J$ = 7.7, 3.1 Hz, 2H, Indole-H 4A/ 4B), 8.02 (dd, $J$ = 7.0, 3.7 Hz, 2H, Indole-H 7A/ 7B), 7.89 (d, $J$ = 7.2 Hz, 2H, Ar-H), 7.66–7.74 (m, 4H, Indole-H (5,6A/ 5,6B)), 7.45 (d, $J$ = 7.0 Hz, 2H, Ar-H), 4.73 (s, 2H, $CH_2$-S); $^{13}$C NMR (150 MHz, DMSO $d_6$): $\delta$ 178.4, 174.7, 161.3, 160.4, 158.7, 157.9, 154.7, 153.8, 152.4, 151.3, 151.0, 148.8, 146.9, 145.9, 145.5, 139.5, 139.2, 137.7, 137.3, 136.9, 134.7, 134.2, 133.4, 130.5, 129.2, 127.2, 42.9; HREI-MS: $m/z$ calcld for $C_{27}H_{18}N_6O_3S$, $[M]^+$ 506.2390 Found 506.2354.

*2.3.9. 1-(4-chlorophenyl)-2-((5,6-di(1H-Indol-3-yl)-1,2,4-triazin-3-yl)thio)ethan-1-one (9)*

Light green, $^1$H NMR (600 MHz, DMSO $d_6$): $\delta$ 12.47 (s, 2H, N–H), 8.74 (s, 2H, Indole-H (2A/ 2B)), 8.62 (dd, $J$ = 7.2, 3.5 Hz, 2H, Indole-H 4A/ 4B), 8.32 (dd, $J$ = 7.6, 3.0 Hz, 2H, Indole-H 7A/ 7B), 7.95 (d, $J$ = 7.0 Hz, 2H, Ar-H), 7.78–7.83 (m, 4H, Indole-H (5,6A/ 5,6B)), 7.61 (d, $J$ = 6.4 Hz, 2H, Ar-H), 4.82 (s, 2H, $CH_2$-S); $^{13}$C NMR (150 MHz, DMSO $d_6$): $\delta$ 184.7, 179.8, 165.6, 165.2, 163.8, 159.9, 159.7, 158.8, 158.2, 157.4, 154.7, 152.6, 150.7, 146.3, 145.6, 143.4, 142.8, 142.7, 142.3, 141.9, 139.7, 139.2, 138.3, 136.6, 133.4, 135.2, 41.8; HREI-MS: $m/z$ calcld for $C_{27}H_{18}ClN_5OS$, $[M]^+$ 495.0260 Found 495.0224.

*2.3.10. 1-(3-bromo-5-chlorophenyl)-2-((5,6-di(1H-Indol-3-yl)-1,2,4-triazin-3-yl)thio)ethan-1-one (10)*

Light green, $^1$H NMR (600 MHz, DMSO $d_6$): $\delta$ 12.50 (s, 2H, N–H), 8.75 (s, 2H, Indole-H (2A/ 2B)), 8.71 (dd, $J$ = 8.0, 3.4 Hz, 2H, Indole-H 4A/ 4B), 8.65 (dd, $J$ = 7.2, 3.0 Hz, 2H, Indole-H 7A/ 7B), 7.94–8.02 (m, 4H, Indole-H (5,6A/ 5,6B)), 7.81 (s, 1H, Ar-H), 7.72 (s, 1H, Ar-H), 7.69 (s, 1H, Ar-H), 4.79 (s, 2H, $CH_2$-S); $^{13}$C NMR (150 MHz, DMSO $d_6$): $\delta$ 179.9, 175.8, 161.6, 160.9, 158.8, 155.2, 155.8, 154.8, 154.4, 153.4, 150.5, 147.1, 145.6, 141.3, 140.7, 139.2, 138.8, 138.7, 138.3, 138.0, 135.7, 135.4, 133.2, 131.6, 128.6, 118.2, 47.8; HREI-MS: $m/z$ calcld for $C_{27}H_{17}BrClN_5OS$, $[M]^+$ 574.5279 Found 574.5250.

*2.3.11. 1-(3-bromo-4-methoxyphenyl)-2-((5,6-di(1H-Indol-3-yl)-1,2,4-triazin-3-yl)thio)ethan-1-one (11)*

Light brown, $^1$H NMR (600 MHz, DMSO $d_6$): $\delta$ 12.44 (s, 2H, N–H), 8.45 (s, 2H, Indole-H (2A/ 2B)), 8.76 (dd, $J$ = 7.9, 2.1 Hz, 2H, Indole-H 4A/ 4B), 7.69 (dd, $J$ = 7.2, 3.4 Hz, 2H, Indole-H 7A/ 7B), 7.64 (s, 1H, Ar-H), 7.61–7.68 (m, 4H, Indole-H (5,6A/ 5,6B)), 7.37 (d, $J$ = 7.1 Hz, 1H, Ar-H), 7.21 (d, $J$ = 7.8 Hz, 1H, Ar-H), 4.47 (s, 2H, $CH_2$-S) 3.97 (s, 3H, $OCH_3$); $^{13}$C NMR (150 MHz, DMSO $d_6$): $\delta$ 182.7, 177.5, 163.3, 162.7, 158.6, 157.9, 157.6, 156.6, 156.4, 154.2, 152.5, 149.1, 147.4, 143.3, 142.8, 141.2, 140.7, 140.6, 140.3, 140.0, 137.5, 137.5, 135.6, 133.6, 133.6, 121.2, 59.5, 44.8; HREI-MS: $m/z$ calcld for $C_{28}H_{20}BrN_5O_2S$, $[M]^+$ 570.4236 Found 570.4203.

*2.3.12. 1-(3-bromo-4-chlorophenyl)-2-((5,6-di(1H-Indol-3-yl)-1,2,4-triazin-3-yl)thio)ethan-1-one (12)*

Light brown, $^1$H NMR (600 MHz, DMSO $d_6$): $\delta$ 12.52 (s, 2H, N–H), 8.58 (s, 2H, Indole-H (2A/ 2B)), 8.55 (dd, $J$ = 7.6, 3.2 Hz, 2H, Indole-H 4A/ 4B), 7.73 (dd, $J$ = 7.0, 3.9 Hz, 2H, Indole-H 7A/ 7B), 7.58 (s, 1H, Ar-H), 7.67–7.74 (m, 4H, Indole-H (5,6A/ 5,6B)), 7.43 (d, $J$ = 8.2 Hz, 1H, Ar-H), 7.38 (d, $J$ = 8.1 Hz, 1H, Ar-H), 4.59 (s, 2H, $CH_2$-S); $^{13}$C NMR (150 MHz, DMSO $d_6$): $\delta$ 186.9, 179.7, 162.3, 160.1, 153.6, 153.4, 150.6, 150.4, 150.0, 148.7, 144.5, 141.6, 140.0, 139.3, 132.8, 132.7, 130.9, 130.8, 130.5, 130.4, 128.8, 128.6, 126.5, 119.6, 119.4, 117.1, 45.5; HREI-MS: $m/z$ calcld for $C_{27}H_{17}BrClN_5OS$, $[M]^+$ 574.3147 Found 574.3125.

## 3. Biological profile

*3.1. 3.1Beta-Glucuronidase inhibitory activity*

The aforementioned synthesized derivatives (**1**–**12**) were evaluated against beta-glucuronidase to investigate the inhibitory potentials and leads to the potent candidates among the series. The inhibitory profiles was compared with standard drug D-saccharic acid 1,4 lactone ($IC_{50}$ = 31.2 ± 1.0 μM). In this var-

**Table 1** Beta-Glucuronidase inhibitory activity and anti-cancer inhibitory activity.

| S/ No | R | $IC_{50}$ (μM ± SEM | $IC_{50}$ Anticancer (mM ± SEM) | S/ No | R | $IC_{50}$ (μM ± SEM | $IC_{50}$ Anticancer (mM ± SEM) |
|---|---|---|---|---|---|---|---|
| **1** | 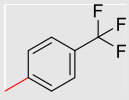 | 5.30 ± 2.0 | 0.80 ± 0.10 | **7** | 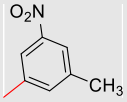 | 21.30 ± 2.0 | 10.0 ± 0.30 |
| **2** | 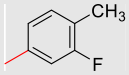 | 15.30 ± 3.0 | 4.02 ± 0.20 | **8** | 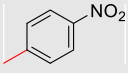 | 8.40 ± 1.0 | 3.60 ± 0.10 |
| **3** | 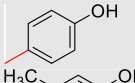 | 7.10 ± 4.0 | 1.40 ± 0.10 | **9** | 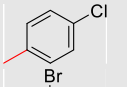 | 7.20 ± 3.0 | 3.80 ± 0.10 |
| **4** | 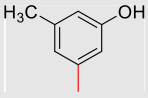 | 19.30 ± 1.0 | 7.10 ± 0.20 | **10** | 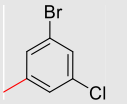 | 29.10 ± 2.0 | 16.20 ± 0.20 |
| **5** | 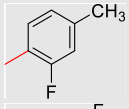 | 13.10 ± 1.0 | 9.10 ± 0.10 | **11** | 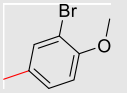 | 33.10 ± 1.0 | 16.20 ± 0.30 |
| **6** | 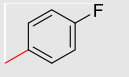 | 6.10 ± 3.0 | 1.80 ± 0.20 | **12** | 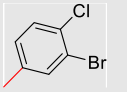 | 29.20 ± 1.0 | 17.20 ± 0.10 |
| **Standard drug** | | | **D-saccharic acid 1,4 lactone ($IC_{50}$ = 31.2 ± 1.0 μM) Tetrandrineb ($IC_{50}$ = 1.37 ± 0.10 μM)** | | | | |

ious substituted derivatives exhibited varied ranges of inhibitory profile ($IC_{50}$ = 5.30 ± 2.0 μM to 33.10 ± 1.0 μM). Number, nature and position of substituents increase and decrease the inhibitory profile. By this analysis various same substituted derivatives were compared in biological inhibitory profiles as well as with standard drug (Table 1).

Based on the presence of different functionalities molecule was represented via different parts in order to compare the biological profiles of the synthesized derivatives. For this purpose structure activity relationships (SAR) were made on the basis of same substituted compounds in order to make the comparison among the analogs (Fig. 1). In this regard analog-**1** ($IC_{50}$ = 5.30 ± 2.0 μM) was found with excellent potential when compared with standard drug D-saccharic acid 1,4 lactone ($IC_{50}$ = 31.2 ± 1.0 μM). The better biological activity of analog-**1** might be the presence of triflouro moiety at *para*-position of aromatic ring. Therefore it was considered as to be much potent analog of the series. Similarly fluoro substituted analogs (**2, 5** and **6**) exhibited significant biological potential such as $IC_{50}$ = 15.30 ± 2.0 μM, $IC_{50}$ = 13.10 ± 1.0 μM and $IC_{50}$ = 6.10 ± 3.0 μM respectively. Among the flouro-substituted analog (**6**) the most effective potential was shown by analog-6 due to the presence of flouro group at *para*-position on aromatic ring which dominantly reduce the enzymatic activity due to much negative charge in the ring by flouro group, while *ortho*-Substituted analog (**2**) found with somewhat lower in potential as compared to analog-**6**. This might be the presence of methyl moiety at *para*-position on aromatic ring. Likewise analog-**5** also contain methyl moiety at *para*-position on aromatic ring and flouro group at *meta*-position which also found with lower in potential due to the presence of methyl group which reduce the biological potential by steric hindrance.

A comparison criterion was set for –OH containing analog-**3** having $IC_{50}$ = 7.10 ± 4.0 μM and analog-**4** with $IC_{50}$ = 19.30 ± 1.0 μM. The significant activity of analog-**3** may be the strong involvement of –OH moiety present at *para*-position while the addition of methyl moiety at *meta*-position of the ring which indicates a clear decline in the activity profile of analog-**4** due to its steric hindrance in the ring. A similar case was observed in $–NO_2$ substituted analogs **7** ($IC_{50}$ = 21.30 ± 2.0 μM) and **8** ($IC_{50}$ = 8.40 ± 1.0 μM) the activity profile was

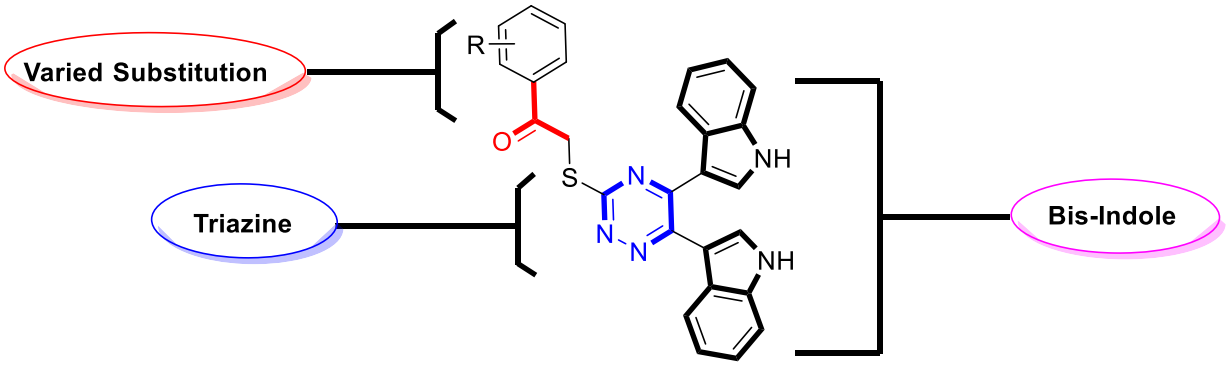


**Fig. 1** General representation of molecule.

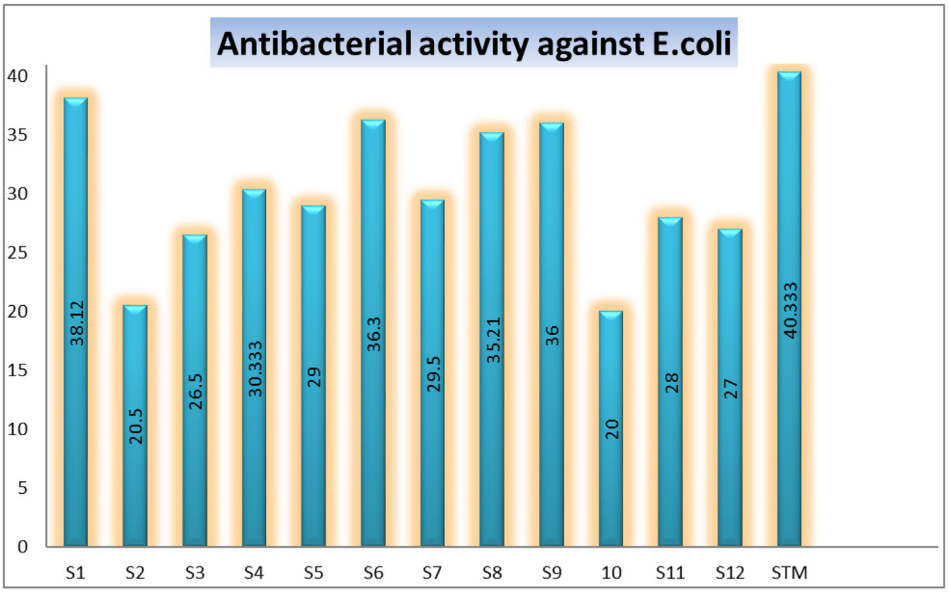


**Graph 1** Represent the anti-bacterial activity of analogs along with streptomycin (STM) a standard drug against *E. coli* specie.

found lower in case of methyl substituted analog-**7** while simple nitro-substituted analog-**8** was found with much better result as compared to standard drug. Moreover, Chloro-substituted analogs-**9** ($IC_{50}$ = 7.20 ± 3.0 μM), **10** ($IC_{50}$ = 2 9.10 ± 2.0 μM) and **12** ($IC_{50}$ = 29.20 ± 1.0 μM) the significant results was found in case of analog-**9** due to the presence of chloro moiety whereas the presence of bromo moiety in case of analog **10** and **12** the inhibitory profile were found somewhat lower than the profile of analog-**9.** This is due to the bulky nature of bromine which reduces the interactive property of molecule thus shown lower potentials. A similar decline was also found in case of –OMe substituted analog-**11** ($IC_{50}$ = 33.10 ± 1.0 μM), due to the presence of bromo group the inhibitory profile was found lower as compare to standard drug.

### *3.2. In vitro anti-cancer inhibitory activity*

All the synthesized analogs (**1**–**12**) were also evaluated for anti-cancer activity in order to investigate the biological inhibitory profile of the potent analog among the synthesized moieties. A similar inhibitory profile was observed when all the analogs were evaluated in the presence of standard drug, Tetrandrineb ($IC_{50}$ = 1.37 ± 0.10 μM). Among the tested series analog-**1**

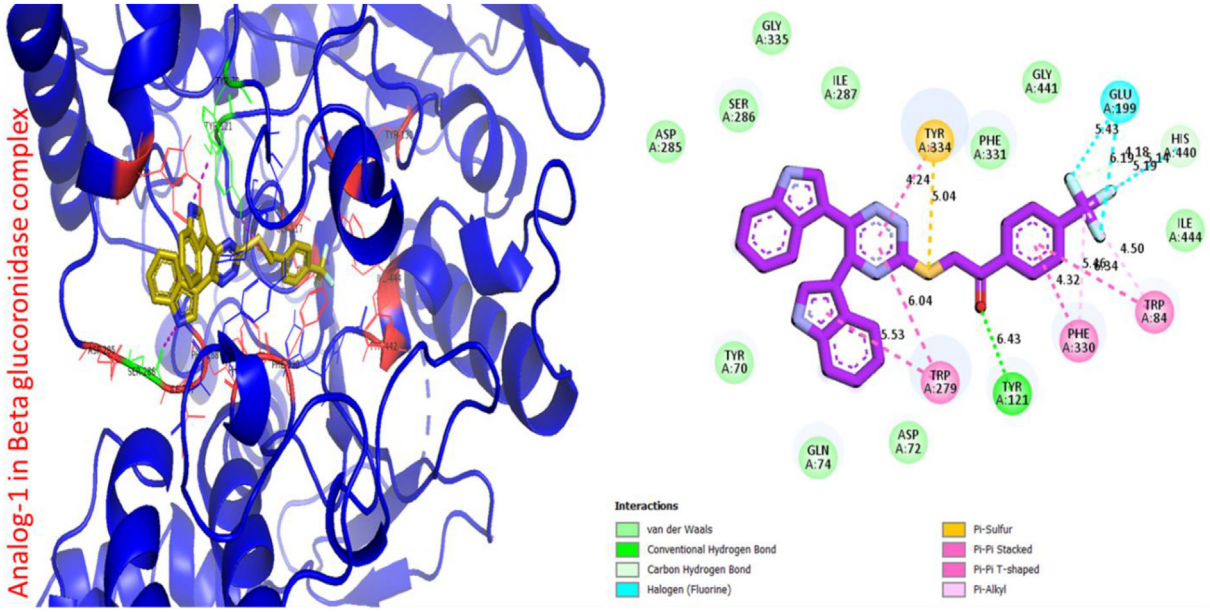


**Fig. 2** Protein ligand interaction (PLI) of analog-1 in beta-glucuronidase complex.

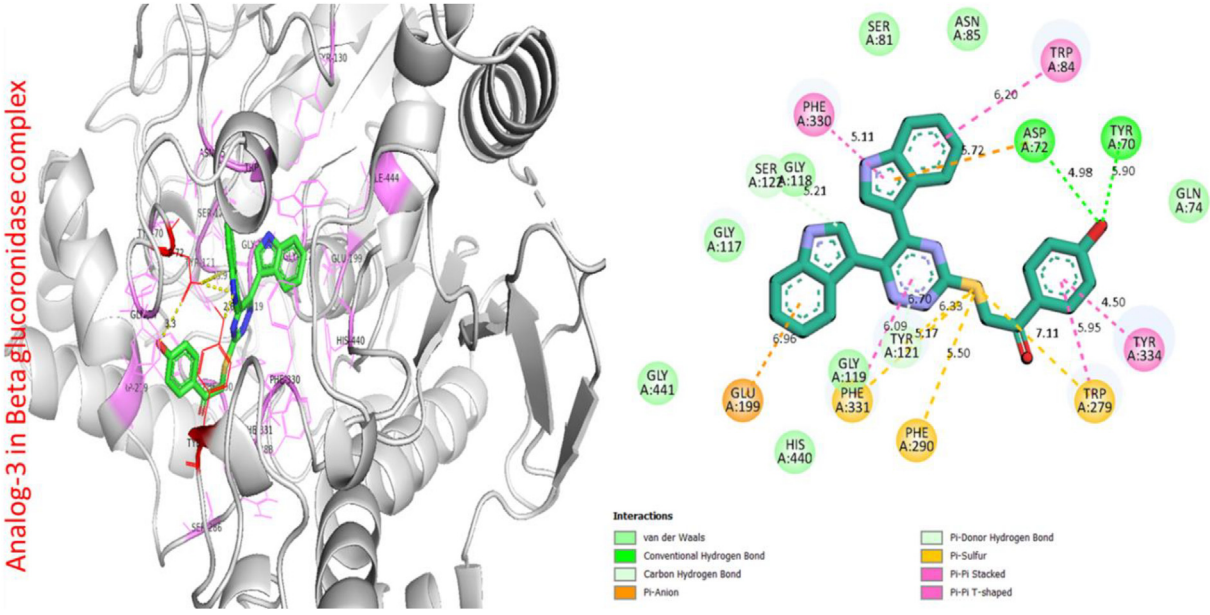


**Fig. 3** Protein ligand interaction (PLI) of analog-3 in beta-glucuronidase complex.

bearing triflouro moiety displayed significant biological activity having $IC_{50}$ = 0.80 ± 0.10 μM. This analog was also found with potent; mention in this activity might be the involvement of flouro groups which might block the enzymatic actions. Moreover, flouro–substituted analogs **2** ($IC_{50}$ = 4.02 ± 0.20 μM), **5** ($IC_{50}$ = 9.10 ± 0.10 μM) and **6** ($IC_{50}$ = 1.80 ± 0.2 0 μM) were comparable activity in this regard, analog bearing only flouro moiety was found to be most effective among the flouro-substituted analogs while the remaining were few fold less potent due to the presence of methyl moiety which decreases the inhibitory profile by its steric hindrance. Likewise –OH containing analogs-**3** ($IC_{50}$ = 1.40 ± 0.10 μM) and **4** ($IC_{50}$ = 7.10 ± 0.20 μM) were also found with remarkable activity profile as compare to standard drug. Both –OH bearing analogs, the potential inhibition was shown by analog-**3**. While analog-**4** was somewhat lower due to the presence of $–CH_3$ group which cause reduction in the inhibitory profile. Nitro-substituted analog-**7** ($IC_{50}$ = 10.0 ± 0.30 μM) and analog-**8** ($IC_{50}$ = 3.60 ± 0.10 μM) also showed moderate to good activity, in this the presence of methyl moiety (analog-**7**) also decrease the activity. A similar decline was also observed in case of chloro-substituted analogs due to the attachment of bromo moiety **10** ($IC_{50}$ = 16.20 ± 0.20 μM) and **12** ($IC_{50}$ = 17.20 ± 0.10 μM) whereas simple chloro-

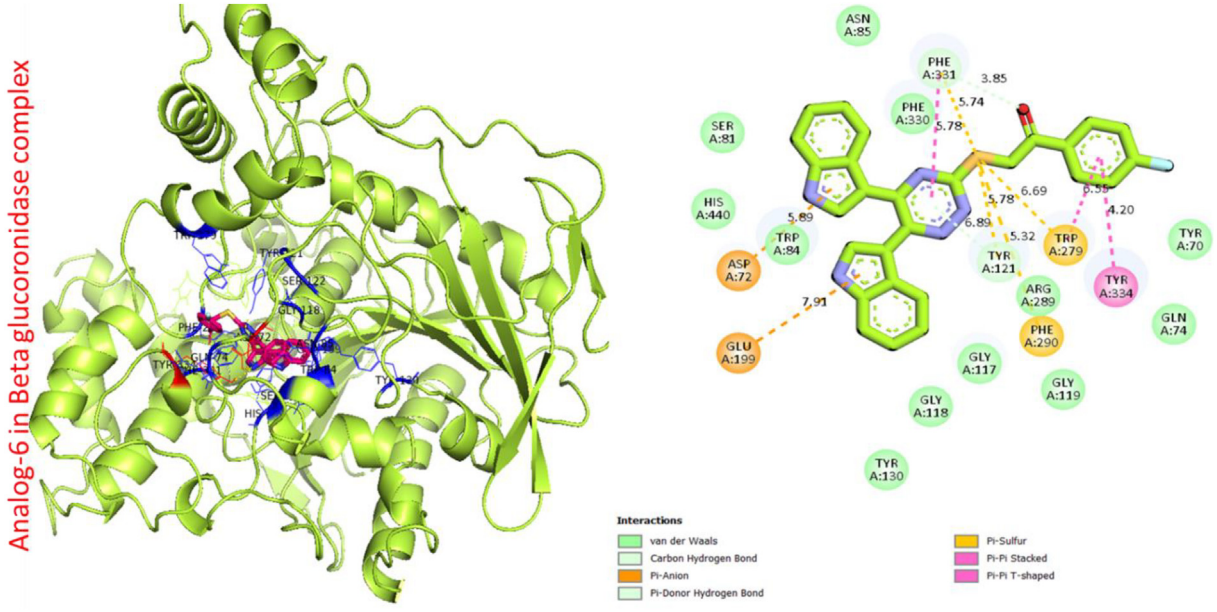


**Fig. 4** Protein ligand interaction (PLI) of analog-6 in beta-glucuronidase complex.

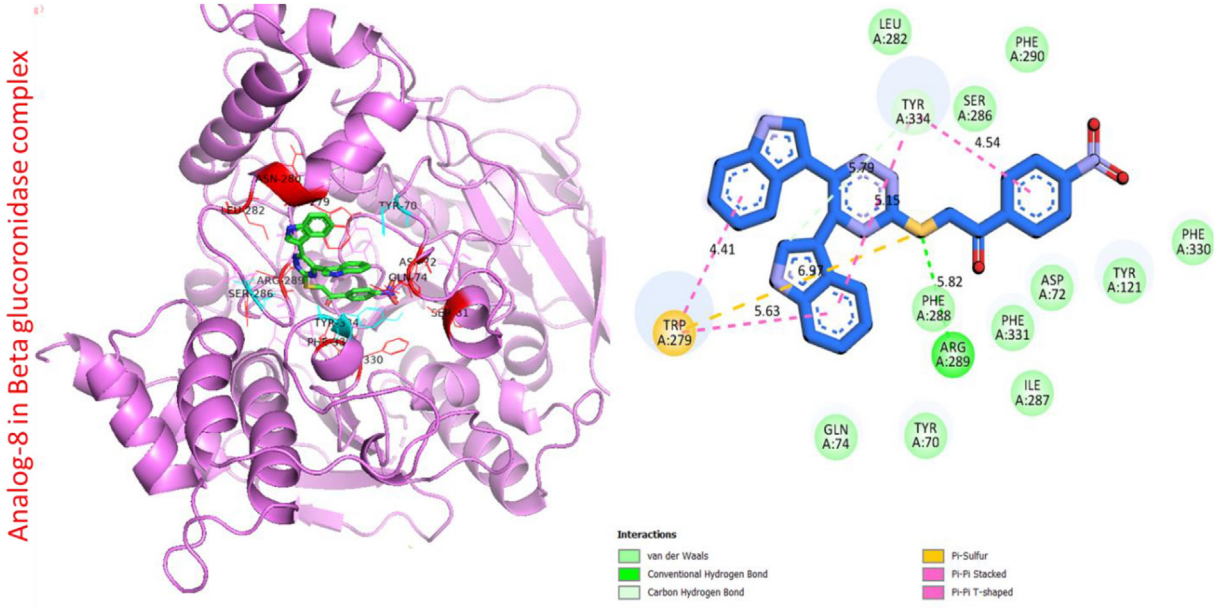


**Fig. 5** Protein ligand interaction (PLI) of analog-8 in beta-glucuronidase complex.

substituted analog-**9** ($IC_{50}$ = 3.80 ± 0.10 μM) was found with better potential. It was concluded that bromo moiety decrease the inhibitory profile due to its bulky nature. Bromo-substituted analog-**11** was also found with lower activity profile which confirms the bulky nature of bromo group that inhibits the inhibitory action of molecules (Table 1).

### 3.3. Anti-bacterial activity

All these compounds were also screened for their inhibitory profile against *E. coli* in order to investigate their anti-bacterial profile. Almost all analogs were found with better to good inhibitory profile but some analogs like **1, 6, 8** and **9** were found with maximum inhibition such as 38.12%, 36.3%, 35.21% and 36% respectively. All the analogs were compared with inhibitory profile of standard drug streptomycin (STM inhibitory profile 40.33%). In this activity it was also concluded that all these analogs having varied substituents which display different inhibitory profile but in this regard the strong inhibition was shown by those analogs having triflouro, hydroxyl, nitro and chloro moieties respectively.

The mechanism related with the insertion of active triflouro group derivatives into the nuclei of *E. Coli* which eventually can bind with DNA and can also suppress the mRNA expression and stop the synthesis of protein results the death of E. Coli cell. Enhanced activity of trifluro group derivatives could be well explained by generation of bonds formed between the active trifluro groups and the peptidoglycan of the cell wall of *E. Coli* and lipoprotein in the outer membrane in addition to blocking the feeding channels which finally results in the death of *E. Coli*.

Due to their effective nature these substituted analogs were maintain their significances as compared to standard drug streptomycin. The excellent potency shown by analog having triflouro group a *para*-position (**1**) of aromatic ring. Inhibitory profiles of these analogs have been incorporated in the graph-1. Form these inhibition it was concluded that position, nature and number of substituents affect the biological activity of analogs. Bulky group reduce the inhibitory profile also observed in this biological activity (Graph 1).

## 4. Docking studies

### 4.1. Docking modes of beta gulcuronidase studies

Molecular docking studies were performed by using Autodock, Discovery Studio Visualizer (DSV) and Pymol. These software were used for different purposes such autodock for molecular docking, DSV and Pymol used for visualization of results (Khan et al., 2023; Khan et al., 2022). Number of compounds were docked and visualized among the potent molecules are listed below (Figs. 2 to 6). In addition, type of receptor, distance and interactions is necessary to visualize the ligand in the protein complex that how the ligand linked to the amino acid with distance due to these reason its interactive tendency can be measured (Elsonbaty et al., 2022; Elsonbaty & Attala 2021; Abdel Raoof et al., 2023; Elsonbaty et al., 2023).

The following potent analogues (**1, 3, 6, 8** and **9)** were found with varied interactions in active sites of enzymes it might be the presence of different substituents such as triflouro, hydroxyl, flouro, nitro and chloro respectively. The better binding interaction of molecules in beta-glucuronidase complex, showed significant results (Table 2).

### 4.2. Docking modes of anticancer studies

Docking studies were also performed for anti-cancer studies against Human ROS1 Kinase Domain. The selected analogs

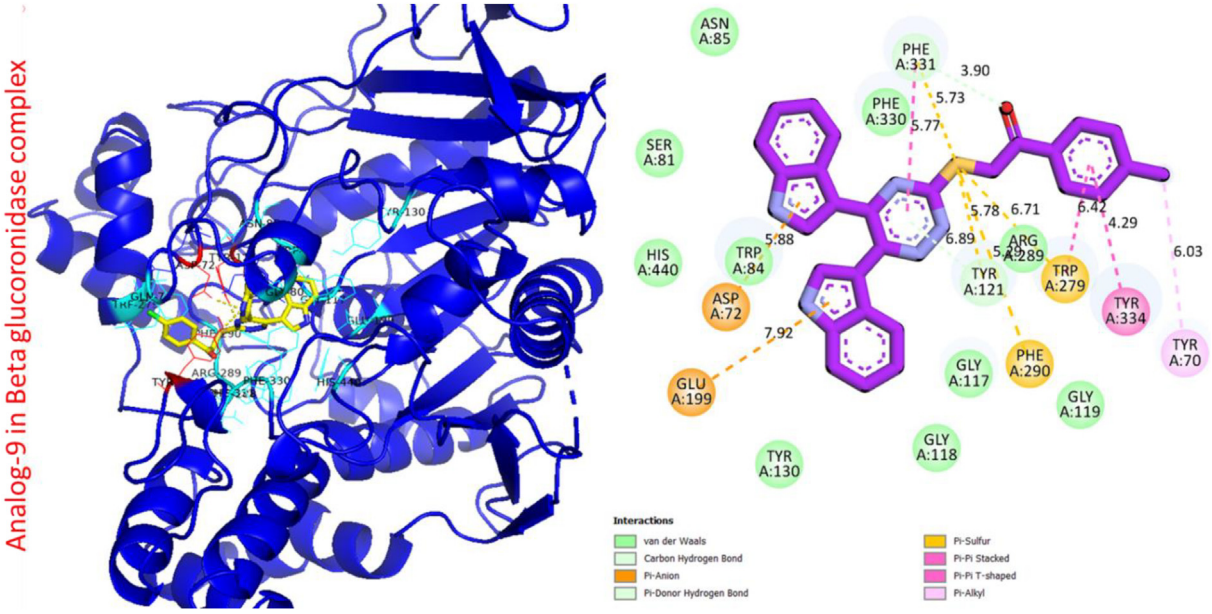


**Fig. 6** Protein ligand interaction (PLI) of analog-9 in beta-glucuronidase complex.

**Table 2** Represent the binding interaction of ligand with active sites of protein (PLI).

| Compound | Receptor | Interaction | Distance | Docking Score |
|---|---|---|---|---|
| Analog 1 in beta-glucuronidase | TRP-A-334 | Pi-S | 4.24A° | −12.6 |
| | TRP-A-334 | Pi-S | 5.04A° | |
| | GLU-A-199 | H-F | 5.43A° | |
| | GLU-A-199 | H-F | 6.19A° | |
| | HIS-A-440 | C-H | 4.18A° | |
| | TRP-A-84 | Pi-Pi Stacked | 4.50A° | |
| | PHE-A-330 | Pi-Pi Stacked | 5.46A° | |
| | PHE-A-330 | Pi-Pi T-Shaped | 4.32A° | |
| | TYR-A-121 | H-B | 6.43A° | |
| | TRP-A-279 | Pi-Pi Stacked | 6.04 A° | |
| | TRP-A-279 | Pi-Pi T-Shaped | 5.53 A° | |
| Analog 3 in beta-glucuronidase | PHE-A-330 | Pi-Pi Stacked | 5.11A° | −11.6 |
| | TRP-A-84 | Pi-Pi Stacked | 6.20A° | |
| | ASP-A-72 | H-B | 5.72A° | |
| | ASP-A-72 | H-B | 4.98A° | |
| | TRP-A-70 | H-B | 5.90A° | |
| | TYR-A-334 | Pi-Pi T-Shaped | 4.50A° | |
| | TRP-A-279 | Pi-S | 5.95A° | |
| | TRP-A-279 | Pi-S | 7.11A° | |
| | PHE-A-290 | Pi-S | 5.95A° | |
| | PHE-A-290 | Pi-S | 6.33A° | |
| | PHE-A-290 | Pi-Pi Stacked | 6.09A° | |
| | GLU-A-199 | Pi-Cation | 6.96 A° | |
| | SER-A-122 | C-H | 5.21A° | |
| Analog 6 in beta-glucuronidase | PHE-A-331 | Pi-Pi Stacked | 5.78A° | −11.4 |
| | PHE-A-331 | Pi-S | 5.74A° | |
| | PHE-A-331 | C-H | 3.85A° | |
| | TYR-A-334 | Pi-Pi Stacked | 4.20A° | |
| | TRP-A-279 | Pi-S | 6.55A° | |
| | TRP-A-279 | Pi-S | 6.69A° | |
| | TYR-A-121 | H-C | 5.32A° | |
| | PHE-A-290 | Pi-S | 5.78A° | |
| | GLU-A-199 | Pi-anion | 7.91A° | |
| | ASP-A-72 | Pi-anion | 5.89A° | |
| Analog 8 in beta-glucuronidase | TRP-A-279 | Pi-S | 6.97A° | −10.2 |
| | TRP-A-279 | Pi-S | 5.63A° | |
| | TRP-A-279 | Pi-S | 4.41A° | |
| | TYR-A-334 | C-H | 5.79A° | |
| | TYR-A-334 | C-H | 5.15A° | |
| | TYR-A-334 | C-H | 4.54A° | |
| | PHE-A-288 | H-B | 5.82A° | |
| Analog 9 in beta-glucuronidase | GLU-A-199 | Pi-Anion | 7.92A° | −9.8 |
| | ASP-A-72 | Pi-Anion | 5.88A° | |
| | PHE-A-331 | C-H | 5.73A° | |
| | PHE-A-331 | C-H | 5.77A° | |
| | TYR-A-70 | Pi-R | 6.03A° | |
| | TYR-A-334 | Pi-Pi-Stacked | 4.29A° | |
| | TRP-A-279 | Pi-Pi-T Shaped | 6.42A° | |
| | TRP-A-279 | Pi-S | 6.71A° | |
| | TYR-A-121 | Pi donor H-B | 6.89A° | |
| | PHE-A-290 | Pi-S | 5.29A° | |
| D_Saccharic acid 1,4 lactone in beta-glucuronidase | TYR-A-175 | H-B | 4.30A | −5.4 |
| | GLN-A-202 | H-B | 4.08A | |
| | PHE-A-200 | Polar H-B | 4.08A | |
| | HIS-A-94 | H-B | 3.67A | |
| | HIS-A-94 | H-B | 3.67A | |

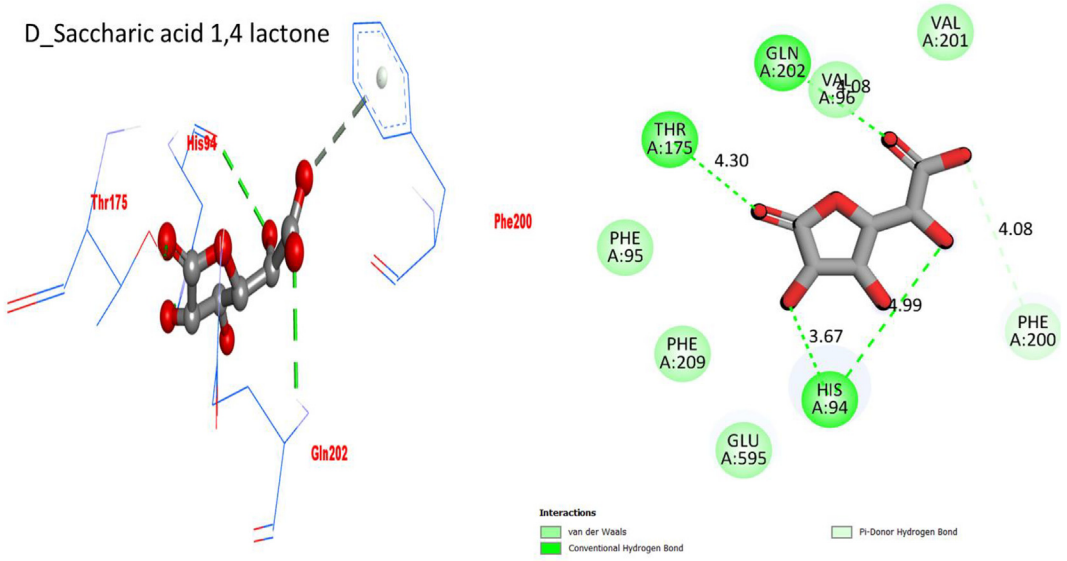


**Fig. 7** Protein ligand interaction (PLI) D_saccharic acid 1,4 lactone in beta-glucuronidase complex.

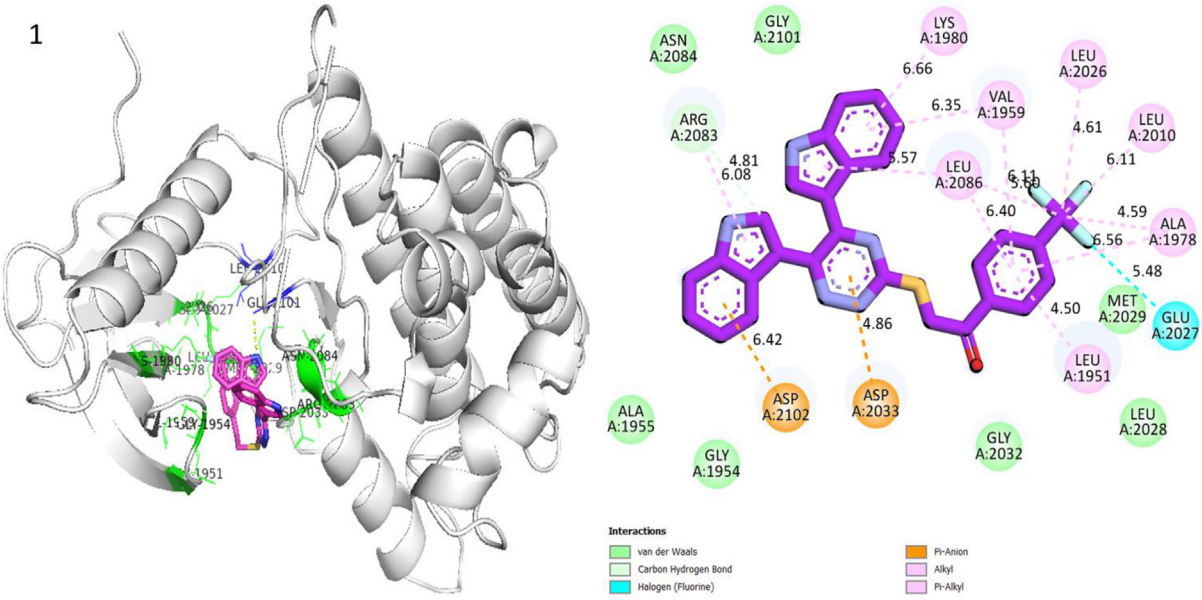


**Fig. 8** Protein ligand interaction (PLI) of analog-1 in Human ROS1 Kinase Domain.

were also subjected in this study to explore the binding interactions of ligand with active site of enzyme (Figs. 7 to 11). The following candidate (**1,3,6,8** and **9**) and their interaction are incorporated in Table 3.(See Fig. 12).

## 5. ADME results

Most of the drugs failed during clinical development had inadequacies in ADME/Tox. Therefore, the purpose of virtual screening should not only be to increase selectivity and enhance binding affinity, but also to consider pharmacokinetic factors as important filters (Khan et al., 2023). Using Qikprop (QikProp, version 3.5, Schrödinger), 44 descriptors and pharmaceutically important characteristics of substituted bis-indole based triazine analogues were examined. Some of the key terms need to envision molecules' drug-like characteristics are reported. Most synthetic compounds have complied with Lipinski's requirements, which are as follows: molecular weight 500, octanol/water partition coefficient (QPlogPo/w), $< 5$ hydrogen bond acceptor $< 10$ and donor $< 5$. For the majority of the derivatives, the oral absorption rate was determined to be between 80 and 100% are shown in graph-2–5. The potent analogs (1,6,8 and 9) were identified for log Kp, Lipinski, Ghose, Veber, Egan, Muegge, Bioavailability, Pains, Brenk, Leadlikensee and synthetic accessibility via ADME study (Graph 2 Graph 3 Graph 4 Graph 5 Graph 6). ADME properties help us to predict the properties of specific molecules which shows drug like properties.

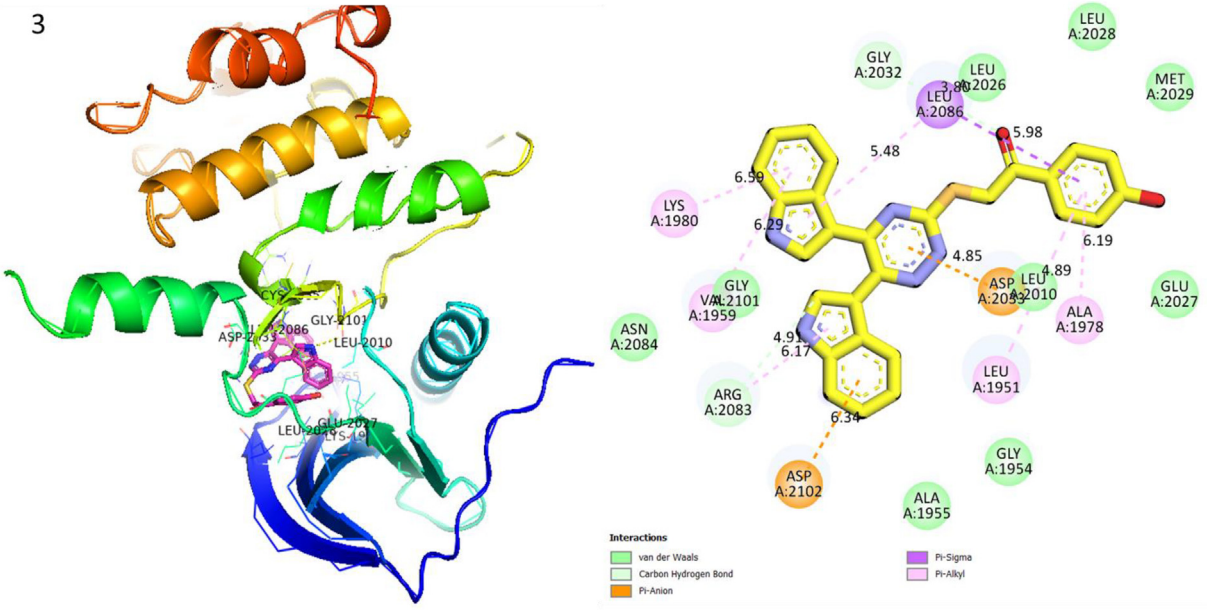


**Fig. 9** Protein ligand interaction (PLI) of analog-3 in Human ROS1 Kinase Domain.

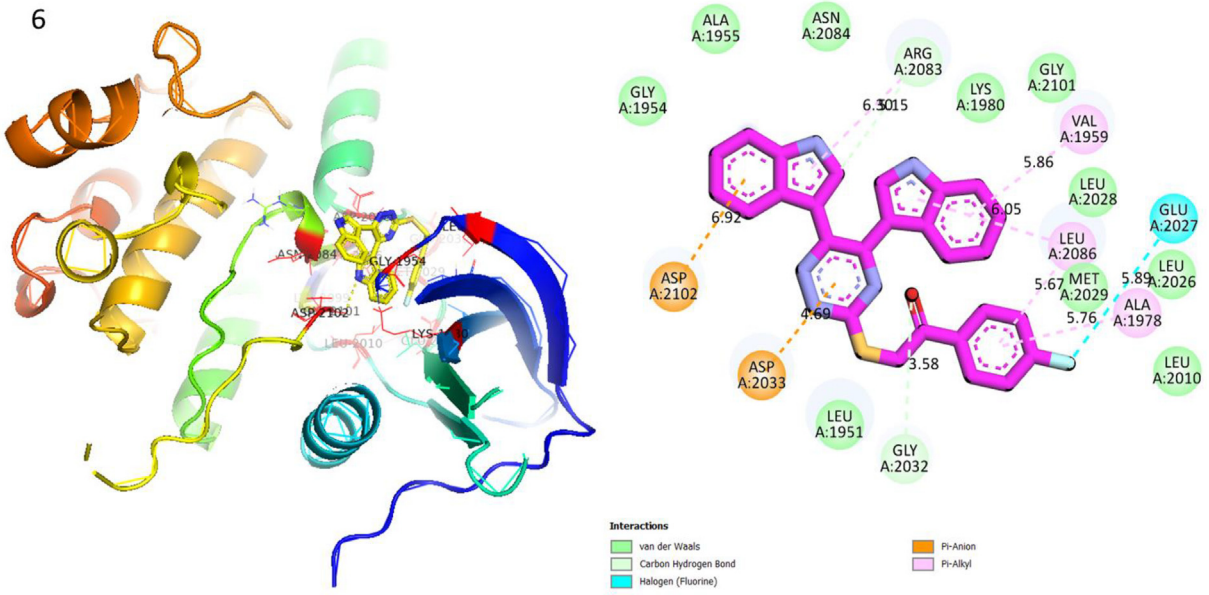


**Fig. 10** Protein ligand interaction (PLI) of analog-6 in Human ROS1 Kinase Domain.

## 6. Conclusion

It was observed form the targeted compounds that nature, number and position of substituents has a great impact on the properties of analogs. Hence in this study we have synthesized, characterized and evaluated for B-glucuronidase, anti-cancer and anti-bacterial activities. Almost all analogs were found with significant results but few analogs such as **1** (2-((5,6-di(1H-indol-3-yl)-1,2,4-triazin-3-yl)thio)-1-(4-(trifluoromethyl)phenyl)ethan-1-one)**, 3** (2-((5,6-di(1H-indol-3-yl)-1,2,4-triazin-3-yl)thio)-1-(4-hydroxyphenyl)ethan-1-one) **6** (2-((5,6-di(1H-indol-3-yl)-1,2,4-triazin-3-yl)thio)-1-(4-fluorophenyl)ethan-1-one)**, 8** (2-((5,6-di(1H-indol-3-yl)-1,2,4-triazin-3-yl)thio)-1-(4-nitrophenyl)ethan-1-one) and **9** (1-(4-chlorophenyl)-2-((5,6-di(1H-indol-3-yl)-1,2,4-triazin-3-yl)thio)ethan-1-one), showed much potent potentials as compared to standard drugs ($_D$-saccharic acid 1,4 lactone, Tetrandrineb and Streptomycin). Moreover, these selected analogs were further subjected for ADME analysis and molecular docking studies in which the physiochemical properties and binding interactions were explored respectively. Finally, it was concluded that the above mention analogs, compound-**1,** was the most effective inhibitor might be the efficacy of

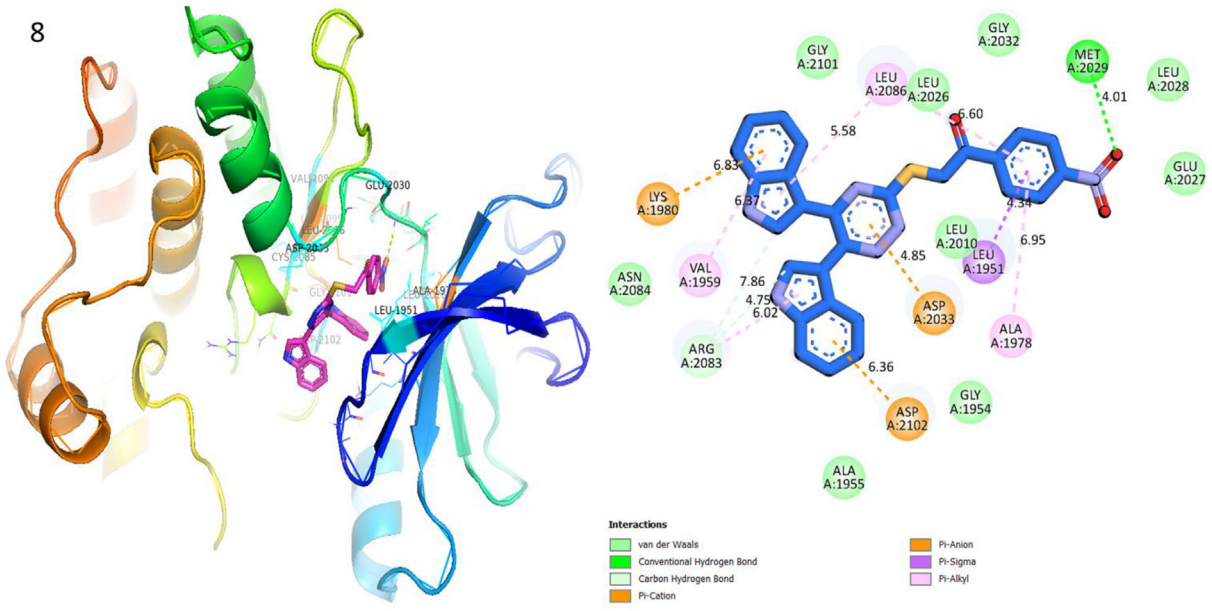


**Fig. 11** Protein ligand interaction (PLI) of analog-8 in Human ROS1 Kinase Domain.

**Table 3** Binding interactions of ligand with active site of enzyme.

| Compound | Receptor | Interaction | Distance | Docking Score |
|---|---|---|---|---|
| Analog 1 in Human ROS1 Kinase Domain | ARG-A-2083 | C-H | 4.81A° | −8.6 |
| | LYS-A-1980 | Pi-R | 6.66A° | |
| | VAL-A-1959 | Pi-R | 6.35A° | |
| | VAL-A-1959 | Pi-R | 6.11A° | |
| | LEU-A-2086 | R | 5.57A° | |
| | LEU-A-2086 | R | 6.40A° | |
| | LEU-A-2026 | Pi-R | 4.61A° | |
| | LEU-A-2010 | Pi-R | 6.11A° | |
| | ALA-A-1978 | Pi-R | 4.59A° | |
| | ALA-A-1979 | Pi-R | 6.56 A° | |
| | GLU-A-2277 | H –F | 5.48 A° | |
| | LEU-A-1951 | Pi-R | 4.50A° | |
| | ASP-A-2033 | Pi-Anion | 4.86A° | |
| | ASP-A-2102 | Pi-Anion | 6.42A° | |
| Analog 3 in Human ROS1 Kinase Domain | LYS-A-1980 | Pi-R | 6.99A° | −8.3 |
| | VAL-A-1959 | Pi-R | 6.29A° | |
| | ARG-A-2083 | H-C | 4.91A° | |
| | ASP-A-2102 | Pi-Anion | 6.34A° | |
| | ASP-A-2033 | Pi-Anion | 4.85A° | |
| | LEU-A-1951 | Pi-R | 4.89A° | |
| | ALA-A-1978 | Pi-R | 6.19A° | |
| | LEU-A-2086 | Pi-Sigma | 5.98A° | |
| | LEU-A-2086 | Pi-Sigma | 5.48A° | |
| Analog 6 in Human ROS1 Kinase Domain | ASP-A-2102 | Pi-Anion | 6.92A° | −7.9 |
| | ASP-A-2033 | Pi-Anion | 4.69A° | |
| | GLY-A-1951 | C-H | 3.58A° | |
| | GLU-A-2077 | H-F | 5.89A° | |
| | TLA-A-1978 | Pi-R | 5.76A° | |
| | LEU-A-2086 | Pi-R | 5.67A° | |
| | LEU-A-2086 | Pi-R | 5.05A° | |
| | VAL-A-1959 | Pi-R | 5.86A° | |
| | ARG-A-2083 | Pi-anion | 6.15A° | |
| Analog 8 in Human ROS1 Kinase Domain | LYS-A-1980 | Pi- anion | 6.83A° | −8.2 |
| | VAL-A-1959 | Pi-R | 6.37A° | |
| | ARG-A-2083 | C-H | 4.75A° | |
| | ASP-A-2102 | Pi- anion | 6.36A° | |

**Table 3** (*continued*)

| Compound | Receptor | Interaction | Distance | Docking Score |
|---|---|---|---|---|
| | ASP-A-2033 | Pi- anion | 4.85A° | |
| | LEU-A-1951 | Pi- Sigma | 4.34A° | |
| | ALA-A-1978 | Pi- R | 6.95A° | |
| | MET-A-2029 | H-B | 4.01A° | |
| | LEU-A-2026 | C-H | 6.60A° | |
| | LEU-A-2086 | Pi- R | 5.58A° | |
| Analog 9 in Human ROS1 Kinase Domain | ASP-A-2102 | Pi-Anion | 6.33A° | −7.3 |
| | ASP-A-2033 | Pi-Anion | 4.89A° | |
| | GLY-A-2032 | C-H | 3.83A° | |
| | LEU-A-1951 | Pi-R | 4.86A° | |
| | ALA-A-1978 | Pi-R | 6.22A° | |
| | LEU-A-2086 | Pi-Sigma | 4.29A° | |
| | LEU-A-2086 | Pi-Sigma | 5.48A° | |
| | VAL-A-1959 | Pi-R | 6.23A° | |
| | LYS-A-1980 | Pi-R | 6.54A° | |
| | ARG-A-2083 | C-H | 5.01A° | |
| | ARG-A-2083 | C-H | 6.26A° | |

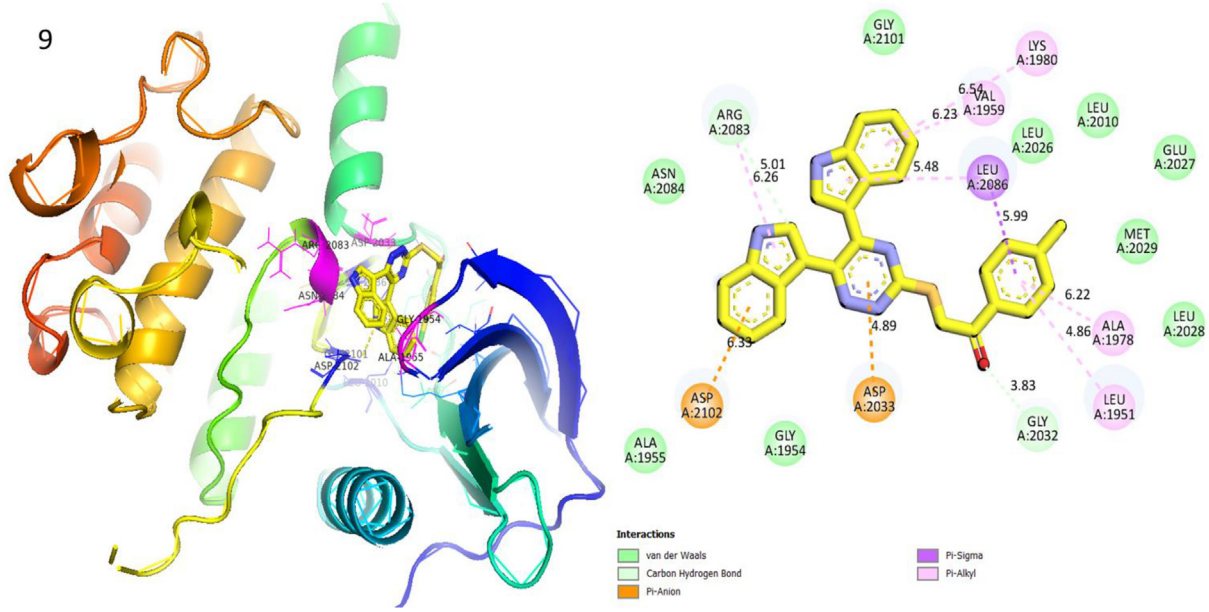


**Fig. 12** Protein ligand interaction (PLI) of analog-9 in Human ROS1 Kinase Domain.

triflouro group, given ranked-1. The other compounds (**3, 6, 8 and 9**) being strong inhibitory profile were also ranked based on their inhibitory activity. Moreover, these compounds were found few folds better profile when compared to their referenced drugs.

## Funding

This work was supported by Princess Nourah bint Abdulrahman University researchers supporting project number (PNURSP2023R205), Princess Nourah bint Abdulrahman University, Riyadh, Saudi Arabia. This work was supported by the Researchers Supporting Project number (RSPD2023R620), King Saud University, Riyadh, Saudi Arabia.

## Declaration of Competing Interest

The authors declare that they have no known competing financial interests or personal relationships that could have appeared to influence the work reported in this paper.

## Acknowledgment

The authors extend their appreciation to the Researchers Supporting Project number (RSPD2023R620), King Saud University, Riyadh, Saudi Arabia. The authors also extend their appreciation to Princess Nourah bint Abdulrahman University researcher supporting project number (PNURSP2023R205), Princess Nourah bint Abdulrahman University, Riyadh, Saudi Arabia.

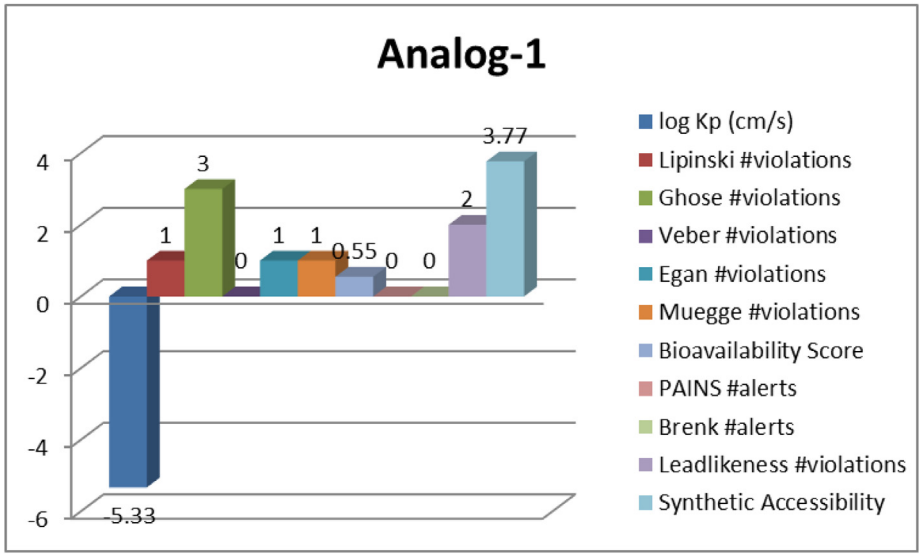


**Graph 2** Represent the ADME properties of the synthesized analog-1.

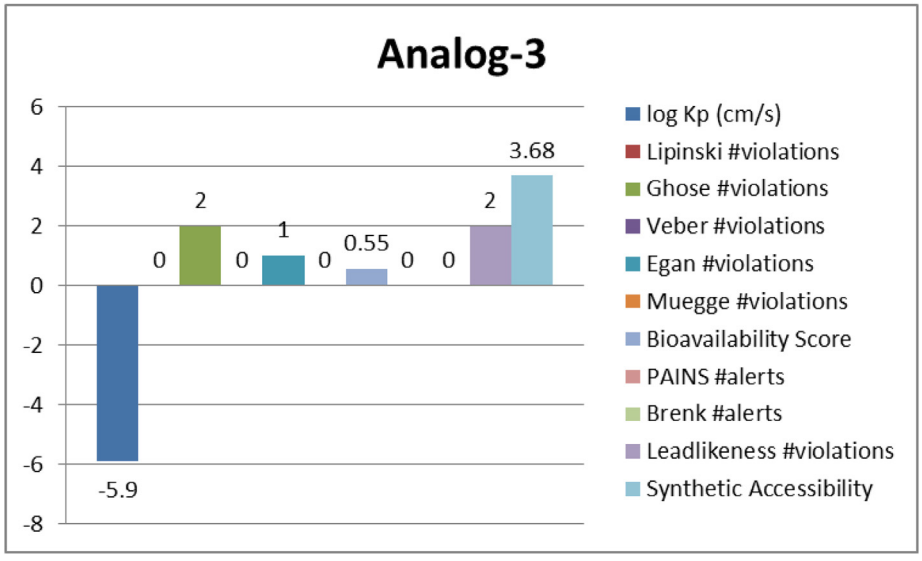


**Graph 3** Represent the ADME properties of the synthesized analog-3.

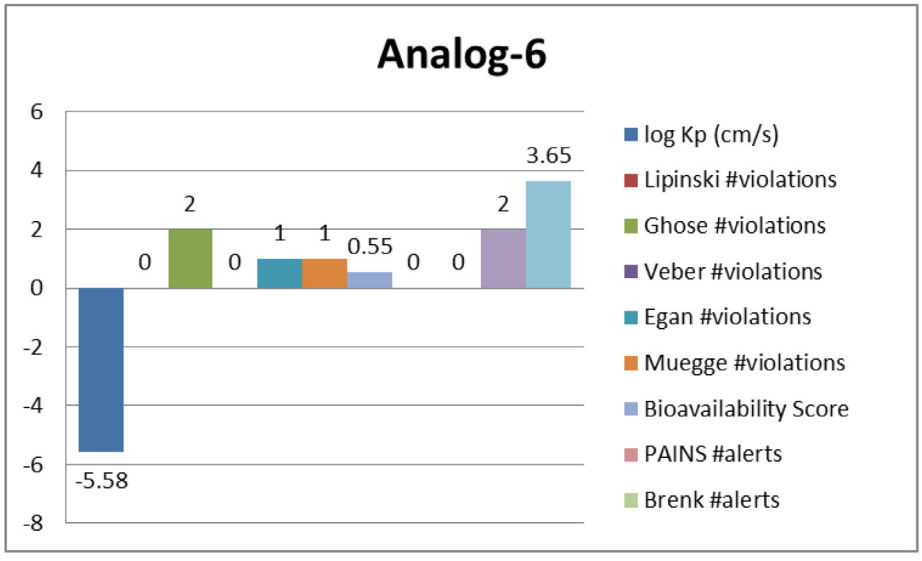


**Graph 4** Represent the ADME properties of the synthesized analog-6.

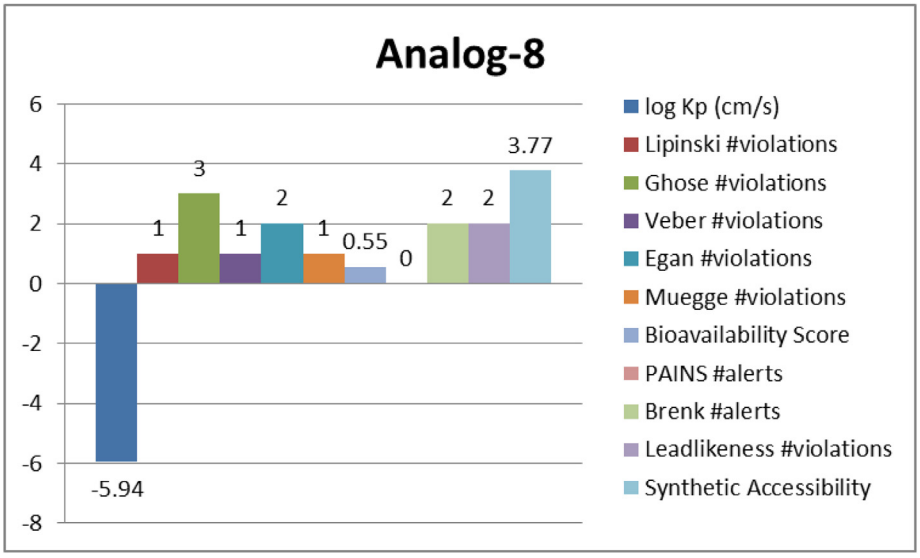


**Graph 5** Represent the ADME properties of the synthesized analog-8.

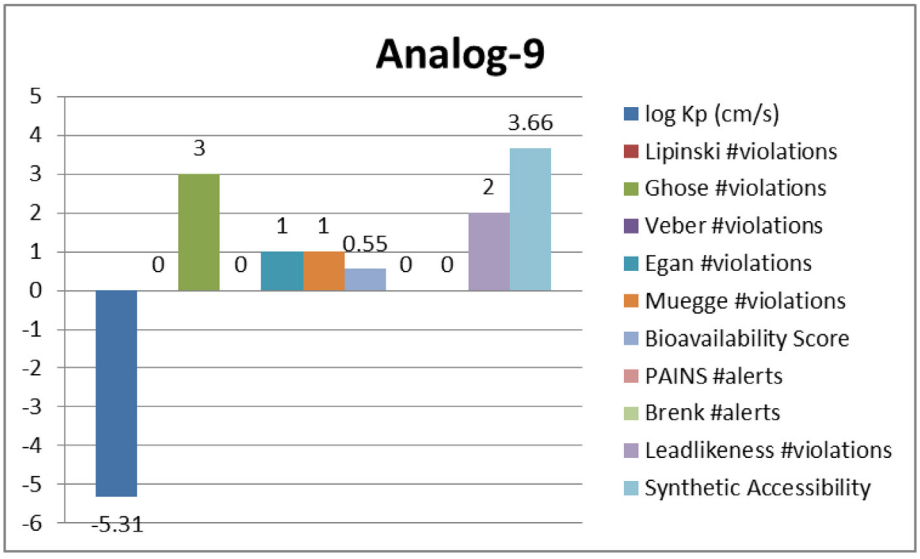


**Graph 6** Represent the ADME properties of the synthesized analog-9.

## References


Abdel-Rahman, R.M., Makki, M.S., Ali, T.E., Ibrahim, M.A., 2015. 1, 2, 4-triazine chemistry part IV: synthesis and chemical behavior of 3-functionalized 5, 6-diphenyl-1, 2, 4-triazines towards some nucleophilic and electrophilic reagents. J. Heterocycl. Chem. 52 (6), 1595–1607.

Abdel-Raoof, A.M., Fouad, M.M., Rashed, N.S., Hosni, N.Y., Elsonbaty, A., Abdel-Fattah, A., 2023. Potentiometric determination of mebeverine hydrochloride antispasmodic drug based on molecular docking with different ionophores host–guest inclusion as a theoretical study. RSC Adv. 13 (2), 1085–1093.

Adalat, B., Rahim, F., Rehman, W., Ali, Z., Rasheed, L., Khan, Y., Farghaly, T.A., Shams, S., Taha, M., Wadood, A., Shah, S.A., 2023. Biologically potent Benzimidazole-based-substituted benzaldehyde derivatives as potent inhibitors for Alzheimer's disease along with molecular docking study. Pharmaceuticals 16 (2), 208.

Byass, P., 2014. The global burden of liver disease: a challenge for methods and for public health. BMC Med. 12 (1), 1–3.

Cacchi, S., Fabrizi, G., 2005. Synthesis and functionalization of indoles through palladium-catalyzed reactions. Chem. Rev. 105 (7), 2873–2920.

Cheng, T.C., Roffler, S.R., Tzou, S.C., Chuang, K.H., Su, Y.C., Chuang, C.H., Kao, C.H., Chen, C.S., Harn, I.H., Liu, K.Y., Cheng, T.L., 2012. An activity-based near-infrared glucuronide trapping probe for imaging β-glucuronidase expression in deep tissues. J. Am. Chem. Soc. 134 (6), 3103–3110.

Chojnowska, S., Kępka, A., Szajda, S.D., Waszkiewicz, N., Bierć, M., Zwierz, K., 2011. Exoglycosidase markers of diseases. Biochem. Soc. Trans. 39, 406–409.

Dadashpour, S., Emami, S., 2018. Indole in the target-based design of anticancer agents: a versatile scaffold with diverse mechanisms. Eur. J. Med. Chem. 150, 9–29.

Elsonbaty, A., Abdel-Raoof, A.M., Abdulwahab, S., Hassan, W.S., Eissa, M.S., 2021. Electrochemical determination of amprolium hydrochloride in chicken meats and eggs: food safety control and theoretical study. J. Electrochem. Soc. 168, (3) 037518.

Elsonbaty, A., Attala, K., 2021. Application of experimental design approaches and in silico molecular docking on the host-guest complexes with Cyclodextrin for the analysis of Benazepril hydrochloride in pharmaceutical formulation. J. Electrochem. Soc. 168, (5) 057515.

Elsonbaty, A., Madkour, A.W., Abdel-Raoof, A.M., Abdel-Monem, A.H., El-Attar, A.A.M., 2022. Computational design for eco-friendly visible spectrophotometric platform used for the assay of the antiviral agent in pharmaceutical dosage form. Spectrochim. Acta Part A: Mol. Biomol. Spectrosc. 271, 120897.

Elsonbaty, A., Attala, K., Eissa, M.S., Abdelshakour, M.A., Mostafa, A.E., Abdel Salam, R.A., Hadad, G.M., 2023. Current advances in computer-aided design of electrochemical sensors: an analytical review. Records Pharma. Biomed. Sci. 7 (1), 65–96.

Falkenbach, A., Wigand, R., Unkelbach, U., Jörgens, K., Martinovic, A., Scheuermann, E.H., Seiffert, U.B., Kaltwasser, J.P., 1993. Cyclosporin treatment in rheumatoid arthritis is associated with an increased serum activity of β-glucuronidase. Scand. J. Rheumatol. 22 (2), 83–85.

Goyal, D., Kaur, A., Goyal, B., 2018. Benzofuran and indole: promising scaffolds for drug development in Alzheimer's disease. ChemMedChem. 13 (13), 1275–1299.

Hassan, M.I., Waheed, A., Grubb, J.H., Klei, H.E., Korolev, S., Sly, W.S., 2013. High resolution crystal structure of human β-glucuronidase reveals structural basis of lysosome targeting. PLoS One 8 (11), e79687.

Hussain, R., Shah, M., Iqbal, S., Rehman, W., Khan, S., Rasheed, L., Naz, H., Al-Ghulikah, H.A., Elkaeed, E.B., Pashameah, R.A. and Alzahrani, E., 2022. Molecular iodine-promoted oxidative cyclization for the synthesis of 1, 3, 4-thiadiazole-fused-[1, 2, 4]-thiadiazole incorporating 1, 4-benzodioxine moiety as potent inhibitors of α-amylase and α-glucosidase: In vitro and in silico study. *Frontiers in Chemistry*, *10*.

Hussain, R., Iqbal, S., Shah, M., Rehman, W., Khan, S., Rasheed, L., Rahim, F., Dera, A.A., Kehili, S., Elkaeed, E.B., Awwad, N.S., 2022. Synthesis of novel Benzimidazole-based Thiazole derivatives as multipotent inhibitors of α-Amylase and α-Glucosidase. in vitro evaluation along with molecular docking study. Molecules 27 (19), 6457.

Imran, S., Taha, M., Hadiani Ismail, N., 2015. A review of bisindolylmethane as an important scaffold for drug discovery. Curr. Med. Chem. 22 (38), 4412–4433.

Juan, T.Y., Roffler, S.R., Hou, H.S., Huang, S.M., Chen, K.C., Leu, Y.L., Prijovich, Z.M., Yu, C.P., Wu, C.C., Sun, G.H., Cha, T.L., 2009. Antiangiogenesis targeting tumor microenvironment synergizes glucuronide prodrug antitumor activity. Clin. Cancer Res. 15 (14), 4600–4611.

Khan, Y., Iqbal, S., Shah, M., Maalik, A., Hussain, R., Khan, S., Khan, I., Pashameah, R.A., Alzahrani, E., Farouk, A.E., Alahmdi, M.I., 2022. New quinoline-based triazole hybrid analogs as effective inhibitors of α-amylase and α-glucosidase: preparation, in vitro evaluation, and molecular docking along with in silico studies. Front. Chem. 10.

Khan, S., Iqbal, S., Khan, M., Rehman, W., Shah, M., Hussain, R., Rasheed, L., Khan, Y., Dera, A.A., Pashameah, R.A., Alzahrani, E., 2022. Design, synthesis, in silico testing, and in vitro evaluation of Thiazolidinone-based Benzothiazole derivatives as inhibitors of α-Amylase and α-Glucosidase. Pharmaceuticals 15 (10), 1164.

Khan, S., Iqbal, S., Rahim, F., Shah, M., Hussain, R., Alrbyawi, H., Rehman, W., Dera, A.A., Rasheed, L., Somaily, H.H., Pashameah, R.A., 2022. New biologically hybrid pharmacophore Thiazolidinone-based indole derivatives: synthesis, in vitro alpha-amylase and alpha-glucosidase along with molecular docking investigations. Molecules 27 (19), 6564.

Khan, S., Iqbal, S., Shah, M., Rehman, W., Hussain, R., Rasheed, L., Alrbyawi, H., Dera, A.A., Alahmdi, M.I., Pashameah, R.A., Alzahrani, E., 2022. Synthesis, in vitro anti-microbial analysis and molecular docking study of aliphatic hydrazide-based benzene sulphonamide derivatives as potent inhibitors of α-glucosidase and urease. Molecules 27 (20), 7129.

Khan, S., Iqbal, S., Taha, M., Rahim, F., Shah, M., Ullah, H., Bahadur, A., Alrbyawi, H., Dera, A.A., Alahmdi, M.I., Pashameah, R.A., 2022. Synthesis, In vitro biological evaluation and in silico molecular docking studies of indole based thiadiazole derivatives as dual inhibitor of acetylcholinesterase and butyrylchloinesterase. Molecules 27 (21), 7368.

Khan, S., Iqbal, S., Rehman, W., Hussain, N., Hussain, R., Shah, M., Ali, F., Fouda, A.M., Khan, Y., Dera, A.A., Alahmdi, M.I., 2023. Synthesis, Molecular docking and ADMET studies of bis-benzimidazole-based thiadiazole derivatives as potent inhibitors, in vitro α-amylase and α-glucosidase. Arab. J. Chem., 104847

Khan, K.M., Rahim, F., Halim, S.A., Taha, M., Khan, M., Perveen, S., Mesaik, M.A., Choudhary, M.I., 2011. Synthesis of novel inhibitors of β-glucuronidase based on benzothiazole skeleton and study of their binding affinity by molecular docking. Bioorg. Med. Chem. 19 (14), 4286–4294.

Khan, Y., Rehman, W., Hussain, R., Khan, S., Malik, A., Khan, M., Liaqat, A., Rasheed, L., Begum, F., Fazil, S., Khan, I., 2022. New biologically potent benzimidazole-based-triazole derivatives as acetylcholinesterase and butyrylcholinesterase inhibitors along with molecular docking study. J. Heterocycl. Chem. 59, 2225–2239.

Khan, S., Ullah, H., Rahim, F., Nawaz, M., Hussain, R., Rasheed, L., 2022. Synthesis, in vitro α-amylase, α-glucosidase activities and molecular docking study of new benzimidazole bearing thiazolidinone derivatives. J. Mol. Struct. 1269, 133812.

Khan, S., Ullah, H., Rahim, F., Taha, M., Hussain, R., Khan, M.S., Ali, H., Khan, M.U., Shah, S.A.A., Khan, K.M., 2022. New thiazole-based thiazolidinone derivatives: synthesis, in vitro α-amylase, α-glucosidase activities and silico molecular docking study. Chem. Data Collect. 42, 100967.

Khan, S., Rahim, F., Rehman, W., Nawaz, M., Taha, M., Fazil, S., Hussain, R., Shah, S.A.A., Abdellatif, M.H., 2022. New benzoxazole-based sulphonamide hybrids analogs as potent inhibitors of α-amylase and α-glucosidase: synthesis and in vitro evaluation along with in silico study. Arab. J. Chem. 15, (12) 104341.

Khan, S., Ullah, H., Taha, M., Rahim, F., Sarfraz, M., Iqbal, R., Iqbal, N., Hussain, R., Shah, S.A.A., Ayub, K., Albalawi, M.A., 2023. Synthesis, DFT studies, molecular docking and biological activity evaluation of thiazole-sulfonamide derivatives as potent Alzheimer's inhibitors. Molecules 28 (2), 559.

Kim, D.H., Jin, Y.H., 2001. Intestinal bacterial β-glucuronidase activity of patients with colon cancer. Archives Pharma. Res. 24, 564–567.

Mumtaz, S., Iqbal, S., Shah, M., Hussain, R., Rahim, F., Rehman, W., Khan, S., Abid, O.U.R., Rasheed, L., Dera, A.A., Al-ghulikah, H. A., 2022. New Triazinoindole bearing Benzimidazole/Benzoxazole hybrids analogs as potent inhibitors of urease: synthesis, in vitro analysis and molecular docking studies. Molecules 27 (19), 6580.

Mürdter, T.E., Friedel, G., Backman, J.T., McClellan, M., Schick, M., Gerken, M., Bosslet, K., Fritz, P., Toomes, H., Kroemer, H.K., Sperker, B., 2002. Dose optimization of a doxorubicin prodrug (HMR 1826) in isolated perfused human lungs: low tumor pH promotes prodrug activation by β-glucuronidase. J. Pharmacol. Exp. Ther. 301 (1), 223–228.

Naz, H., Islam, A., Waheed, A., Sly, W.S., Ahmad, F., Hassan, M.I., 2013. Human β-glucuronidase: structure, function, and application in enzyme replacement therapy. Rejuvenation Res. 16 (5), 352–363.

Prakash, B., Amuthavalli, A., Edison, D., Sivaramkumar, M.S., Velmurugan, R., 2018. Novel indole derivatives as potential anticancer agents: design, synthesis and biological screening. Med. Chem. Res. 27, 321–331.

Singh, T.P., Singh, O.M., 2018. Recent progress in biological activities of indole and indole alkaloids. Mini Rev. Med. Chem. 18 (1), 9–25.

Sravanthi, T.V., Manju, S.L., 2016. Indoles—a promising scaffold for drug development. Eur. J. Pharm. Sci. 91, 1–10.

Szajda, S.D., Jankowska, A., Zwierz, K., 2008. Carbohydrate markers in colon carcinoma. Dis. Markers 25 (4–5), 233–242.

Zalewska-Szajda, B., Taranta-Janusz, K., Chojnowska, S., Waszkiewicz, N., Zwierz, K., Wasilewska, A., 2018. Urinary exoglycosidases, reference values in healthy children. Adv. Med. Sci. 63 (2), 224–229.